DOI: 10.1051/epjconf/201716300034

Fission barriers from multidimensionally-constrained covariant density functional theories

Bing-Nan Lu[1,2], *Jie* Zhao[1,3], *En-Guang* Zhao[1,4], and *Shan-Gui* Zhou[1,4,5,6,⋆]

[1] *CAS Key Laboratory of Frontiers in Theoretical Physics, Institute of Theoretical Physics, Chinese Academy of Sciences, Beijing 100190, China*
[2] *Institut für Kernphysik (IKP-3) and Jülich Center for Hadron Physics, Forschungszentrum Jülich, D-52425 Jülich, Germany*
[3] *Microsystem and Terahertz Research Center, China Academy of Engineering Physics, Chengdu 610200, China*
[4] *Center of Theoretical Nuclear Physics, National Laboratory of Heavy Ion Accelerator, Lanzhou 730000, China*
[5] *School of Physical Sciences, University of Chinese Academy of Sciences, Beijing 100049, China*
[6] *Synergetic Innovation Center for Quantum Effects and Application, Hunan Normal University, Changsha, 410081, China*

Abstract. In recent years, we have developed the multidimensionally-constrained covariant density functional theories (MDC-CDFTs) in which both axial and spatial reflection symmetries are broken and all shape degrees of freedom described by $\beta_{\lambda\mu}$ with even μ, such as $\beta_{20}, \beta_{22}, \beta_{30}, \beta_{32}, \beta_{40}$, etc., are included self-consistently. The MDC-CDFTs have been applied to the investigation of potential energy surfaces and fission barriers of actinide nuclei, third minima in potential energy surfaces of light actinides, shapes and potential energy surfaces of superheavy nuclei, octupole correlations between multiple chiral doublet bands in ^{78}Br, octupole correlations in Ba isotopes, the Y_{32} correlations in $N = 150$ isotones and Zr isotopes, the spontaneous fission of Fm isotopes, and shapes of hypernuclei. In this contribution we present the formalism of MDC-CDFTs and the application of these theories to the study of fission barriers and potential energy surfaces of actinide nuclei.

1 Introduction

Many intrinsic nuclear shapes which break certain spatial symmetries play important roles in determining nuclear structure and fission properties [1–5]. The nuclear shape can be described by parametrizing the nuclear surface or the nucleon density distribution with the multipole expansion method. The deformation is then characterized by the expansion coefficient $\beta_{\lambda\mu}$.

Although the axial quadrupole (β_{20}) shape are prevalent in nuclear physics study, there have become more and more theoretical and experimental investigations on the β_{22} deformation, which manifests itself in the wobbling motion [2, 6], chiral doublet bands [7–11] and the termination of rotational bands [12], and the β_{30} deformation, which is characterized by parity doublet bands [13–15]. The impact of the non-axial octupole (β_{32}) deformation on the low-lying spectra have been also a hot topic in last decades [16–25].

Since the discovery of the fission phenomena [26], a quantitative description of the whole fission process has been very challenging. It was already known that the fission dynamics are mostly determined by the barriers prohibiting the dissolving of the nucleus [27]. Thus for solving the fission problem, one needs very accurate information on fission barriers, e.g., the heights.

Due to the shell effects, many actinide nuclei are found to be characterized by the two-humped fission barrier [28–37]. Consequently any models concerning the fission phenomena should be able to reproduce the barrier heights with certain assumptions on the nuclear shapes. For example, in early calculations of the fission barriers, the nuclei are usually assumed to be axially symmetric. Later it was found that the occurrence of the triaxial and the octupole deformations has non-negligible consequences in determining the heights of the inner and outer fission barriers, respectively. It has been known from the macroscopic-microscopic model calculations that the inner fission barrier is lowered when the triaxial deformation is allowed, so is the outer one by the reflection asymmetric distortion [30, 31]. Such lowering effects were also revealed in the non-relativistic [35] and relativistic [38, 39] density functional calculations, respectively. Recently, it is shown in Ref. [40] that the outer barriers are further lowered by the triaxial deformation compared with axially symmetric results. This lowering effect for the reflection-asymmetric outer barrier is of 0.5~1 MeV, accounting for 10%~20% of the barrier height. It is thus necessary to include these shape degrees of freedom properly in any systematic calculations.

To study nuclear ground states, shape isomers and PES's, it is desirable to have microscopic and self-consistent models in which all known important shape degrees of freedom are included. We have developed such

⋆e-mail: sgzhou@itp.ac.cn

a model, the so called multidimensionally-constrained covariant density functional theories (MDC-CDFTs), by breaking the reflection and axial symmetries simultaneously.

In MDC-CDFTs, the nuclear shape is assumed to be invariant under the reversion of x and y axes, i.e., the intrinsic symmetry group is V_4 and all shape degrees of freedom $\beta_{\lambda\mu}$ with even μ (β_{20}, β_{22}, β_{30}, β_{32}, β_{40}, $\cdots$) are included self-consistently. The MDC-CDFTs consist of two types of models: the multidimensionally-constrained relativistic mean field (MDC-RMF) model and the multidimensionally-constrained relativistic Hartree-Bogoliubov (MDC-RHB) model.

In the MDC-RMF model, the BCS approach has been implemented for the particle-particle (pp) channel. This model has been used to study potential energy surfaces and fission barriers of actinides [40–45], the spontaneous fission of several fermium isotopes [46], the Y_{32} correlations in $N = 150$ isotones [47], and shapes of hypernuclei [48, 49], see Refs. [50–52] for recent reviews.

In the MDC-RHB model, pairing correlations are treated by making the Bogoliubov transformation which generalizes the BCS quasi-particle concept and provides a unified description of particle-hole (ph) and pp correlations in a mean-field level. A separable pairing force of finite range [53–57] is adopted. The MDC-RHB model has been used to study the spontaneous fission of fermium isotopes [58], octupole correlations between multiple chiral doublet (MχD) bands in ^{78}Br [59], octupole correlations in Ba isotopes [15] and the Y_{32} correlations in neutron-rich Zr nuclei [60].

In this contribution, we present briefly the formalism of the MDC-CDFTs and some results of fission barriers. The formulae of the MDC-CDFTs is given in Sec. 2. The results and discussions are presented in Sec. 3. Finally we summarize in Sec. 4.

2 Formalism

In the CDFT [61–70], there are four types of covariant density functionals: the meson exchange or point-coupling nucleon interactions combined with the nonlinear or density dependent couplings [71–77] (see Ref. [78] for recent reviews). In this contribution we only show the CDFT with non-linear point coupling (NL-PC) interactions.

The starting point of the relativistic NL-PC density functional is the following Lagrangian:

$$\mathcal{L} = \bar{\psi}(i\gamma_\mu\partial^\mu - M_B)\psi - \mathcal{L}_{\rm lin} - \mathcal{L}_{\rm nl} - \mathcal{L}_{\rm der} - \mathcal{L}_{\rm Cou}, \quad (1)$$

where $M_{\rm B}$ is the nucleon mass and $\mathcal{L}_{\rm lin}$, $\mathcal{L}_{\rm nl}$, $\mathcal{L}_{\rm der}$ and $\mathcal{L}_{\rm Cou}$ are the linear coupling, non-linear coupling, derivative coupling and the Coulomb part, respectively, see Refs. [50–52] for details. Starting from the Lagrangian, we can deduce the relativistic mean field equations with the variational principle:

$$\{\boldsymbol{\alpha}\cdot\boldsymbol{p} + \beta\,[M_B + S(\boldsymbol{r})] + V(\boldsymbol{r})\}\,\psi_k(\boldsymbol{r}) = \epsilon_k\psi_k(\boldsymbol{r}), \quad (2)$$

where $S(\boldsymbol{r})$ and $V(\boldsymbol{r})$ are the scalar and vector potentials, respectively. As usual we suppose that the states are invariant under the time-reversal operation, which means that all time-odd components of the currents and the potentials vanish.

The pairing correlations play an important role in the fission process [79, 80]. We have implemented the BCS method or the Bogoliubov transformation for pairing in the MDC-RMF or MDC-RHB models.

The axially deformed harmonic oscillator (ADHO) basis [81, 82] was adopted in the development of MDC-CDFTs. In contrast to the traditional ADHO code, in this work the components with different quantum numbers are mixed, allowing us to treat triaxial and octupole nuclear shapes simultaneously.

The ADHO basis are defined as the eigensolutions of the Schrödinger equation with an ADHO potential,

$$\left[-\frac{\hbar^2\nabla^2}{2M} + \frac{1}{2}M(\omega_\rho^2\rho^2 + \omega_z^2 z^2)\right]\Phi_\alpha(\boldsymbol{r}\sigma) = E_\alpha\Phi_\alpha(\boldsymbol{r}\sigma), \quad (3)$$

where ω_z and ω_ρ are the oscillator frequencies along and perpendicular to the symmetry axis, respectively. The solution of Eq. (3) reads

$$\Phi_\alpha(\boldsymbol{r}\sigma) = C_\alpha\phi_{n_z}(z)R_{n_\rho}^{m_l}(\rho)\frac{1}{\sqrt{2\pi}}e^{im_l\varphi}\chi_{s_z}(\sigma), \quad (4)$$

where $\phi_{n_z}(z)$ and $R_{n_\rho}^{m_l}(\rho)$ are the HO wave functions, χ_{s_z} is a two component spinor and C_α is a complex number introduced for convenience. These bases are also eigenfunctions of the z component of the angular momentum j_z with eigenvalues $K = m_l + m_s$.

These bases form a complete set for expanding any two-component spinors. For a Dirac spinor with four components, the following expansion can be made,

$$\psi_i(\boldsymbol{r}\sigma) = \begin{pmatrix} \sum_\alpha f_i^\alpha\Phi_\alpha(\boldsymbol{r}\sigma) \\ \sum_\alpha g_i^\alpha\Phi_\alpha(\boldsymbol{r}\sigma) \end{pmatrix}, \quad (5)$$

where the sum runs over all the possible combination of the quantum numbers $\alpha = \{n_z, n_r, m_l, m_s\}$, f_i^α and g_i^α are the expansion coefficients.

In the general case that the axial symmetry as well as the space reflection symmetry are broken, different components with different m_j and π are mixed with each other. In this case it is convenient to choose the operator $\hat{S} = ie^{-i\pi j_z}$ with $S^2 = 1$ as the conserved quantity to classify the energy levels. S is a good quantum number for the basis with $\hat{S}\Phi_\alpha = S\Phi_\alpha = (-1)^{K_\alpha-\frac{1}{2}}\Phi_\alpha$, which means that the bases Φ_α with $K_\alpha = 1/2, -3/2, 5/2, -7/2, \cdots$ span the subspace with $S = 1$, while their time-reversed states span the one with $S = -1$. Note that now the block with $K = 1/2$ should be mixed with that with $K = -3/2$ instead of that with $K = 3/2$.

For deformed nuclei with the V_4 symmetry, we expand the potentials $V(\boldsymbol{r})$ and $S(\boldsymbol{r})$ and the densities in terms of the Fourier series,

$$f(\rho,\varphi,z) = f_0(\rho,z)\frac{1}{\sqrt{2\pi}} + \sum_{n=1}^{\infty} f_n(\rho,z)\frac{1}{\sqrt{\pi}}\cos(2n\varphi). \quad (6)$$

DOI: 10.1051/epjconf/201716300034

The matrix elements of the potentials can then be calculated from the expansion coefficients [42, 60].

In addition to the mean field energy, the centre of mass correction is calculated either phenomenologically or microscopically, depending on which effective interaction is used. The intrinsic multipole moments are calculated from the densities by

$$Q^{\tau}_{\lambda\mu} = \int d^3\boldsymbol{r}\rho^{\tau}_{V}(\boldsymbol{r})r^{\lambda}Y_{\lambda\mu}(\Omega), \tag{7}$$

where $Y_{\lambda\mu}(\Omega)$ is the spherical harmonics and τ refers to the proton, neutron or nucleon. The deformation parameter $\beta_{\lambda\mu}$ is obtained from the corresponding multipole moment by

$$\beta_{\lambda\mu} = \frac{4\pi}{3NR^{\lambda}}Q_{\lambda\mu}, \tag{8}$$

where $R = 1.2 \times A^{1/3}$ fm and N is the number of proton, neutron or nucleons.

3 Results

The double-humped fission barriers of actinide nuclei are often used to benchmark theoretical models for fission barriers. As the nucleus evolves from the ground state to the fission configurations, various shape degrees of freedom play important and different roles in determining the heights of the inner and outer barriers. As mentioned in the introduction, the inner barrier is lowered when the triaxial deformation is allowed, while for the outer barrier, the reflection asymmetric shape is favored. In Ref. [40] we have shown that, the reflection asymmetric outer barrier may be further lowered by the triaxial distortion with the MDC-RMF model.

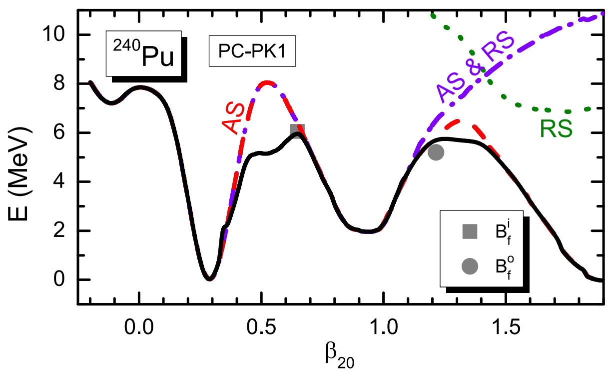

Figure 1. (Color online) Potential energy curves of ^{240}Pu with various self-consistent symmetries imposed. The solid black curve represents the calculated fission path with V_4 symmetry imposed: the red dashed curve that with axial symmetry (AS) imposed, the green dotted curve that with reflection symmetry (RS) imposed, the violet dot-dashed line that with both symmetries (AS & RS) imposed. The empirical inner (outer) barrier height [83] is denoted by the grey square (circle). The energy is normalized with respect to the binding energy of the ground state. The parameter set used is PC-PK1 [84]. Taken from Ref. [40].

In Fig. 1 we show the one-dimensional potential energy curves (PEC) from an oblate shape with β_{20} about −0.2 to the fission configuration with β_{20} beyond 2.0 which are obtained from calculations with different self-consistent symmetries imposed: the axial (AS) or triaxial (TS) symmetries combined with reflection symmetric (RS) or asymmetric (RA) cases. The importance of the triaxial deformation on the inner barrier and that of the octupole deformation on the outer barrier are clearly seen: The triaxial deformation reduces the inner barrier height by more than 2 MeV and results in a better agreement with the empirical value [83]; the RA shape is favored beyond the fission isomer and lowers very much the outer fission barrier. Besides these features, it was found in Ref. [40] that the outer barrier is also considerably lowered by about 1 MeV when the triaxial deformation is allowed. In addition, a better reproduction of the empirical barrier height can be seen for the outer barrier. It has been stressed that this feature can be revealed only when the axial and reflection symmetries are simultaneously broken [40].

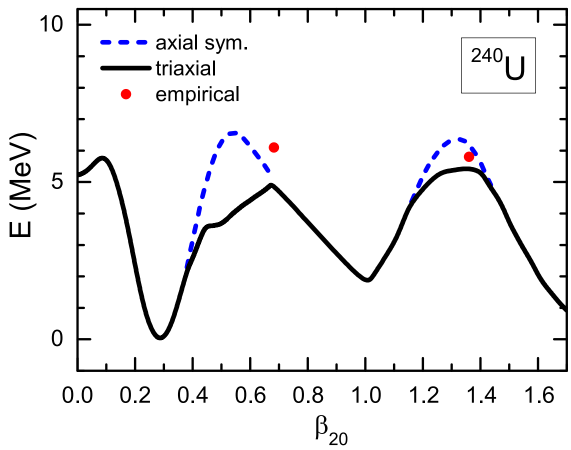

Figure 2. (Color online) Potential energy curves of ^{240}U. The solid black curve represents the calculated fission path with V_4 symmetry imposed, the blue dotted curve represents that with axial symmetry (AS) imposed. The empirical inner barrier height [85] is denoted by the dots. The energy is normalised with respect to the binding energy of the ground state. The parameter set used is PC-PK1 [84].

In Fig. 2 we show the calculated potential energy curves for ^{240}U. The results with and without non-axial deformations are presented. Near the second barrier both the axial and non-axial results are reflection asymmetric. The empirical values of the fission barriers are taken from Ref. [85] and depicted by red dots. The calculated inner and outer fission barrier heights are 4.96 and 5.43 MeV, respectively. This means that in ^{240}U, the outer fission barrier is higher than the inner one, which is in contrast to the empirical values. It's worthwhile to mention that the outer fission barrier height is very close to 5.5 MeV, a value which was recently obtained in JAEA [86]. It is clearly shown that the inclusion of non-axial shapes improve the agreement between the calculation and the experiment.

In Ref. [42] we applied the MDC-RMF model to a systematical study of fission barriers of the actinide nuclei with both axial and reflection symmetries broken. In Fig. 3 we show the calculated potential energy curves near

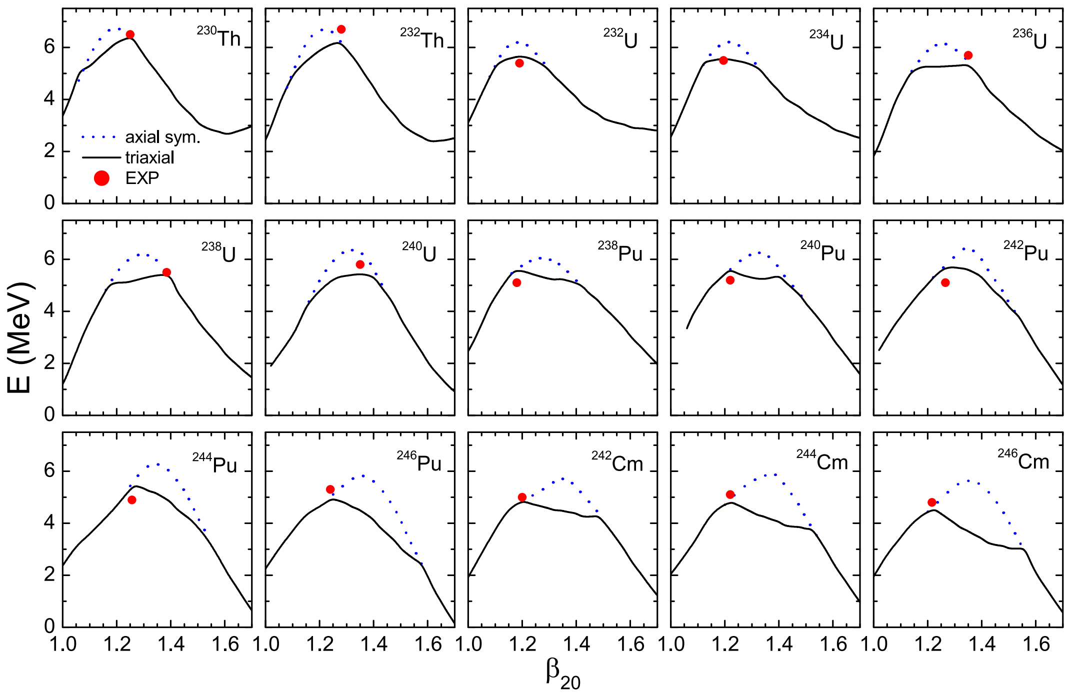

Figure 3. (Color online) Potential energy curves of even-even actinides nuclei in the outer barrier regions from the MDC-RMF calculations. The reflection asymmetric shapes are allowed. The triaxial results are displayed by solid lines, while the results from the axial symmetric calculations are shown by dashed lines. The binding energies are normalized with respect to the binding energies of the ground states of each nucleus. The empirical values of fission barrier heights are shown as red dots [83, 85]. Taken from Ref. [42].

the outer barriers of the actinide nuclei. For comparison the results with and without non-axial deformations are both presented. Note that near the second barrier all the results are reflection asymmetric. Because only the β_{20} deformation is constrained, the total binding energy is automatically minimized against other possible deformation parameters. The empirical values of the fission barriers are depicted by red dots. Clearly, all the axial symmetric calculations overestimate the barrier height. After including the triaxial deformation, the agreement between the calculated values and the empirical ones becomes better.

Besides the double-humped barriers of the PES's in the actinide region, the occurrence of a third barrier at large deformations beyond the second one was predicted by macroscopic-microscopic model calculations in the 1970s. But contradictory results about the existence of the third barrier were later obtained with different models. In Ref. [45] the MDC-RMF model was used to investigate the triple-humped barriers in light even-even actinides ^{232,234,236,238}U and ^{226,228,230,232}Th. The relativistic functionals PC-PK1 [84] and DD-ME2 [87] were adopted. Next we will mainly discuss the results from DD-ME2.

A third minimum was found on the PES's of ^{232,234,238}U: The pocket is rather shallow for ^{232}U and ^{234}U and very pronounced for ^{238}U. These results are quite similar to those obtained in recent calculations based on the macroscopic-microscopic model [88–91] and the Skyrme Hartree-Fock-Bogoliubov model [92].

In the case of Th isotopes, our calculation predicts a pronounced third minimum for ^{226}Th with a pocket depth of 2–3 MeV. As the neutron number N increases, both the energy of the third minimum and the height of the third barrier decrease, and the depth of the third well is also reduced. This trend has also been predicted in macroscopic-microscopic calculations [91]. For ^{230}Th only a shallow pocket of depth less than 1 MeV occurs around the third minimum. The pocket around the third minimum is very shallow for ^{232}Th.

4 Summary

In this contribution we present the formalism and some applications of the MDC-CDFTs in which all shape degrees of freedom $\beta_{\lambda\mu}$ with even μ are allowed. The potential energy surfaces (curves) of actinide nuclei and the effect of the triaxiality on the first and second fission barriers were investigated. It is found that besides the octupole deformation, the triaxiality also plays an important role upon the second fission barriers. The third minimum of actinide nuclei were also studied. A pronounced third minimum were predicted for ^{226}Th with a pocket depth of 2–3 MeV.

Acknowledgments

This work has been supported by the NSF of China (11120101005, 11275248, 11525524, 11621131001, 11647601 and 11711540016), the 973 Program of China (2013CB834400), the Key Research Program of Frontier Sciences of CAS, the HPC Cluster of SKLTP/ITP-CAS and the Supercomputing Center, CNIC of CAS.

References

[1] A. Bohr, B.R. Mottelson, *Nuclear Structure*, Vol. I (World Scientific, Singapore, 1998)

[2] A. Bohr, B.R. Mottelson, *Nuclear Structure*, Vol. II (World Scientific, Singapore, 1998)

[3] P. Ring, P. Schuck, *The Nuclear Many-Body Problem* (Springer-Verlag, Berlin/Heidelberg/New York, 1980)

[4] S. Frauendorf, Rev. Mod. Phys. **73**, 463 (2001)

[5] W. Nazarewicz, in *An Advanced Course in Modern Nuclear Physics (Lecture Notes in Physics)*, edited by J. Arias, M. Lozano (Springer, Berlin/Heidelberg, 2001), Vol. 581, pp. 102–140

[6] S.W. Odegard, G.B. Hagemann, D.R. Jensen, M. Bergstroem, B. Herskind, G. Sletten, S. Toermaenen, J.N. Wilson, P.O. Tjom, I. Hamamoto et al., Phys. Rev. Lett. **86**, 5866 (2001)

[7] S. Frauendorf, J. Meng, Nucl. Phys. A **617**, 131 (1997)

[8] K. Starosta, T. Koike, C.J. Chiara, D.B. Fossan, D.R. LaFosse, A.A. Hecht, C.W. Beausang, M.A. Caprio, J.R. Cooper, R. Krucken et al., Phys. Rev. Lett. **86**, 971 (2001)

[9] J. Meng, J. Peng, S.Q. Zhang, S.G. Zhou, Phys. Rev. C **73**, 037303 (2006)

[10] J. Meng, S.Q. Zhang, J. Phys. G: Nucl. Phys. **37**, 064025 (2010)

[11] J. Meng, S.Q. Zhang, P. Zhao, in *Relativistic Density Functional for Nuclear Structure*, edited by J. Meng (World Scientific Publishing Co. Pte. Ltd., 2016), Vol. 10 of *International Review of Nuclear Physics*, chap. 9. Novel rotational excitations, pp. 355–411

[12] A.V. Afanasjev, D.B. Fossan, G.J. Lane, I. Ragnarsson, Phys. Rep. **322**, 1 (1999)

[13] L.P. Gaffney, P.A. Butler, M. Scheck, A.B. Hayes, F. Wenander, M. Albers, B. Bastin, C. Bauer, A. Blazhev, S. Bonig et al., Nature **497**, 199 (2013)

[14] B. Bucher, S. Zhu, C.Y. Wu, R.V.F. Janssens, D. Cline, A.B. Hayes, M. Albers, A.D. Ayangeakaa, P.A. Butler, C.M. Campbell et al., Phys. Rev. Lett. **116**, 112503 (2016)

[15] X.C. Chen, J. Zhao, C. Xu, H. Hua, T.M. Shneidman, S.G. Zhou, X.G. Wu, X.Q. Li, S.Q. Zhang, Z.H. Li et al., Phys. Rev. C **94**, 021301(R) (2016)

[16] I. Hamamoto, B. Mottelson, H. Xie, X.Z. Zhang, Z. Phys. D **21**, 163 (1991)

[17] J. Skalski, Phys. Rev. C **43**, 140 (1991)

[18] X. Li, J. Dudek, Phys. Rev. C **49**, R1250 (1994)

[19] S. Takami, K. Yabana, M. Matsuo, Phys. Lett. B **431**, 242 (1998)

[20] M. Yamagami, K. Matsuyanagi, M. Matsuo, Nucl. Phys. A **693**, 579 (2001)

[21] J. Dudek, A. Gozdz, N. Schunck, M. Miskiewicz, Phys. Rev. Lett. **88**, 252502 (2002)

[22] J. Dudek, D. Curien, N. Dubray, J. Dobaczewski, V. Pangon, P. Olbratowski, N. Schunck, Phys. Rev. Lett. **97**, 072501 (2006)

[23] P. Olbratowski, J. Dobaczewski, P. Powalowski, M. Sadziak, K. Zberecki, Int. J. Mod. Phys. E **15**, 333 (2006)

[24] K. Zberecki, P. Magierski, P.H. Heenen, N. Schunck, Phys. Rev. C **74**, 051302(R) (2006)

[25] J. Dudek, A. Gozdz, K. Mazurek, H. Molique, J. Phys. G: Nucl. Phys. **37**, 064032 (2010)

[26] O. Hahn, F. Strassmann, Naturwissenschaften **27**, 11 (1939)

[27] N. Bohr, J.A. Wheeler, Phys. Rev. **56**, 426 (1939)

[28] V.M. Strutinsky, Nucl. Phys. A **95**, 420 (1967)

[29] V.M. Strutinsky, Nucl. Phys. A **122**, 1 (1968)

[30] V.V. Pashkevich, Nucl. Phys. A **133**, 400 (1969)

[31] P. Möller, S.G. Nilsson, Phys. Lett. B **31**, 283 (1970)

[32] M. Brack, J. Damgaard, A.S. Jensen, H.C. Pauli, V.M. Strutinsky, C.Y. Wong, Rev. Mod. Phys. **44**, 320 (1972)

[33] T. Burvenich, M. Bender, J.A. Maruhn, P.G. Reinhard, Phys. Rev. C **69**, 014307 (2004)

[34] M. Mirea, L. Tassan-Got, Cent. Eur. J. Phys. **9**, 116 (2011)

[35] M. Girod, B. Grammaticos, Phys. Rev. C **27**, 2317 (1983)

[36] V. Blum, J.A. Maruhn, P.G. Reinhard, W. Greiner, Phys. Lett. B **323**, 262 (1994)

[37] L. Csige, M. Csatlos, T. Faestermann, J. Gulyas, D. Habs, R. Hertenberger, M. Hunyadi, A. Krasznahorkay, H.J. Maier, P.G. Thirolf et al., Phys. Rev. C **85**, 054306 (2012)

[38] H. Abusara, A.V. Afanasjev, P. Ring, Phys. Rev. C **82**, 044303 (2010)

[39] K. Rutz, J.A. Maruhn, P.G. Reinhard, W. Greiner, Nucl. Phys. A **590**, 680 (1995)

[40] B.N. Lu, E.G. Zhao, S.G. Zhou, Phys. Rev. C **85**, 011301(R) (2012)

[41] B.N. Lu, J. Zhao, E.G. Zhao, S.G. Zhou, J. Phys: Conf. Ser. **492**, 012014 (2014)

[42] B.N. Lu, J. Zhao, E.G. Zhao, S.G. Zhou, Phys. Rev. C **89**, 014323 (2014)

[43] B.N. Lu, J. Zhao, E.G. Zhao, S.G. Zhou, Phys. Scr. **89**, 054028 (2014)

[44] B.N. Lu, J. Zhao, E.G. Zhao, S.G. Zhou, EPJ Web Conf. **38**, 05003 (2012)

[45] J. Zhao, B.N. Lu, D. Vretenar, E.G. Zhao, S.G. Zhou, Phys. Rev. C **91**, 014321 (2015)

[46] J. Zhao, B.N. Lu, T. Nikšić, D. Vretenar, S.G. Zhou, Phys. Rev. C **93**, 044315 (2016)

[47] J. Zhao, B.N. Lu, E.G. Zhao, S.G. Zhou, Phys. Rev. C **86**, 057304 (2012)

[48] B.N. Lu, E.G. Zhao, S.G. Zhou, Phys. Rev. C **84**, 014328 (2011)

[49] B.N. Lu, E. Hiyama, H. Sagawa, S.G. Zhou, Phys. Rev. C **89**, 044307 (2014)

[50] L.L. Li, B.N. Lu, N. Wang, K. Wen, C.J. Xia, Z.H. Zhang, J. Zhao, E.G. Zhao, S.G. Zhou, Nucl. Phys. Rev. **31**, 253 (2014), (in Chinese)

[51] B.N. Lu, J. Zhao, E.G. Zhao, S.G. Zhou, in *Relativistic Density Functional for Nuclear Structure*, edited by J. Meng (World Scientific Publishing Co. Pte. Ltd., 2016), Vol. 10 of *International Review of Nuclear Physics*, chap. 5. Superheavy nuclei and fission barriers, pp. 171–217
[52] S.G. Zhou, Phys. Scr. **91**, 063008 (2016)
[53] Y. Tian, Z.Y. Ma, Chin. Phys. Lett. **23**, 3226 (2006)
[54] Y. Tian, Z.Y. Ma, P. Ring, Phys. Lett. B **676**, 44 (2009)
[55] Y. Tian, Z.y. Ma, P. Ring, Phys. Rev. C **80**, 024313 (2009)
[56] T. Nikšić, D. Vretenar, P. Ring, Phys. Rev. C **78**, 034318 (2008)
[57] T. Nikšić, P. Ring, D. Vretenar, Y. Tian, Z.y. Ma, Phys. Rev. C **81**, 054318 (2010)
[58] J. Zhao, B.N. Lu, T. Nikšić, D. Vretenar, Phys. Rev. C **92**, 064315 (2015)
[59] C. Liu, S.Y. Wang, R.A. Bark, S.Q. Zhang, J. Meng, B. Qi, P. Jones, S.M. Wyngaardt, J. Zhao, C. Xu et al., Phys. Rev. Lett. **116**, 112501 (2016)
[60] J. Zhao, B.N. Lu, E.G. Zhao, S.G. Zhou, Phys. Rev. C **95**, 014320 (2017)
[61] B.D. Serot, J.D. Walecka, Adv. Nucl. Phys. **16**, 1 (1986)
[62] P.G. Reinhard, Rep. Prog. Phys. **52**, 439 (1989)
[63] P. Ring, Prog. Part. Nucl. Phys. **37**, 193 (1996)
[64] M. Bender, P.H. Heenen, P.G. Reinhard, Rev. Mod. Phys. **75**, 121 (2003)
[65] D. Vretenar, A.V. Afanasjev, G.A. Lalazissis, P. Ring, Phys. Rep. **409**, 101 (2005)
[66] J. Meng, H. Toki, S.G. Zhou, S.Q. Zhang, W.H. Long, L.S. Geng, Prog. Part. Nucl. Phys. **57**, 470 (2006)
[67] N. Paar, D. Vretenar, G. Colo, Rep. Prog. Phys. **70**, 691 (2007)
[68] T. Nikšić, D. Vretenar, P. Ring, Prog. Part. Nucl. Phys. **66**, 519 (2011)
[69] H. Liang, J. Meng, S.G. Zhou, Phys. Rep. **570**, 1 (2015)
[70] J. Meng, S.G. Zhou, J. Phys. G: Nucl. Part. Phys. **42**, 093101 (2015)
[71] J. Boguta, A.R. Bodmer, Nucl. Phys. A **292**, 413 (1977)
[72] R. Brockmann, H. Toki, Phys. Rev. Lett. **68**, 3408 (1992)
[73] Y. Sugahara, H. Toki, Nucl. Phys. A **579**, 557 (1994)
[74] B.A. Nikolaus, T. Hoch, D.G. Madland, Phys. Rev. C **46**, 1757 (1992)
[75] T. Burvenich, D.G. Madland, J.A. Maruhn, P.G. Reinhard, Phys. Rev. C **65**, 044308 (2002)
[76] C. Fuchs, H. Lenske, H.H. Wolter, Phys. Rev. C **52**, 3043 (1995)
[77] T. Nikšić, D. Vretenar, P. Finelli, P. Ring, Phys. Rev. C **66**, 024306 (2002)
[78] J. Meng, ed., *Relativistic Density Functional for Nuclear Structure*, Vol. 10 of *International Review of Nuclear Physics* (World Scientific Pub Co Pte Lt, 2016)
[79] S. Karatzikos, A.V. Afanasjev, G.A. Lalazissis, P. Ring, Phys. Lett. B **689**, 72 (2010)
[80] A. Bulgac, P. Magierski, K.J. Roche, I. Stetcu, Phys. Rev. Lett. **116**, 122504 (2016)
[81] H. Kucharek, P. Ring, Z. Phys. A **339**, 23 (1991)
[82] P. Ring, Y.K. Gambhir, G.A. Lalazissis, Comput. Phys. Commun. **105**, 77 (1997)
[83] R. Capote, M. Herman, P. Oblozinsky, P.G. Young, S. Goriely, T. Belgya, A.V. Ignatyuk, A.J. Koning, S. Hilaire, V.A. Plujko et al., Nucl. Data Sheets **110**, 3107 (2009)
[84] P.W. Zhao, Z.P. Li, J.M. Yao, J. Meng, Phys. Rev. C **82**, 054319 (2010)
[85] P. Möller, A. J. Sierk, T. Ichikawa, A. Iwamoto, R. Bengtsson, H. Uhrenholt, S. Aberg, Phys. Rev. C **79**, 064304 (2009)
[86] K. Nishio, private communications
[87] G.A. Lalazissis, T. Nikšić, D. Vretenar, P. Ring, Phys. Rev. C **71**, 024312 (2005)
[88] M. Kowal, J. Skalski, Phys. Rev. C **85**, 061302(R) (2012)
[89] P. Jachimowicz, M. Kowal, J. Skalski, Phys. Rev. C **87**, 044308 (2013)
[90] T. Ichikawa, A. Iwamoto, P. Möller, A.J. Sierk, Phys. Rev. C **86**, 024610 (2012)
[91] T. Ichikawa, P. Möller, A.J. Sierk, Phys. Rev. C **87**, 054326 (2013)
[92] J.D. McDonnell, W. Nazarewicz, J.A. Sheikh, Phys. Rev. C **87**, 054327 (2013)